

SCIENTIFIC REPORTS



OPEN

Both air-sea components are crucial for El Niño forecast from boreal spring

Xiang-Hui Fang & Mu Mu

The spring predictability barrier severely limits our ability to forecast the El Niño-Southern Oscillation (ENSO) from and across the boreal spring. Our observational analysis shows that the spring predictability barrier (SPB) can be largely reduced when information from both the ocean and atmosphere are effectively taken into account during the boreal spring. The correlation coefficient between the predicted and observed sea surface temperature anomalies over the equatorial central-eastern Pacific determined by a simple quaternary linear regression model is >0.81 for the period 1980–2016. The frame structure of the ENSO evolution is mostly controlled by variations in the oceanic heat content along the equatorial Pacific and the zonal wind stress over the tropical western Pacific during the boreal spring. These results indicate that to predict ENSO events with a long lead time, i.e., largely reducing the SPB, variations in both the ocean and atmosphere during the boreal spring should be well predicted first. While the oceanic information is mainly located in the equatorial Pacific and well characterized by the delayed oscillator and recharging oscillator models, variations in the atmosphere may contain information beyond this area and are more difficult to deal with.

As the dominant interannual variability, El Niño-Southern Oscillation (ENSO) has far-reaching impacts on climate and society around the world¹. The simulation and forecasting of ENSO is therefore of great importance. As the leading paradigm for the ENSO theory, the recharge oscillator emphasizes the time delay between anomalies in longitudinally averaged thermocline depth (TCD; approximated by the depth of the 20 °C isotherm) and the eastern Pacific (EP) sea surface temperature (SST) and explains the periodic characteristics of ENSO^{2,3}. Analyses of observational data have confirmed this paradigm and have suggested that the oceanic heat content along the equatorial Pacific is a good predictor of the ENSO events⁴. Recent work has indicated that if the changing background state is accounted for, all flavours of El Niño will have similar early subsurface origins⁵. These results emphasize the important part played by the ocean in the ENSO system and suggest that it may be possible to predict ENSO events with a long lead time. However, forecasts of ENSO are limited by the spring predictability barrier (SPB), which refers to a sudden reduction in the ENSO forecast skills across the spring period in most climate models^{4,6–9}. As indicated in ref.¹⁰, the skill of model runs based on observations in the boreal spring to predict the boreal winter SST anomalies averaged over the Niño3.4 region (170° W–120° W, 5° S–5° N) is poor, with a correlation coefficient of about 0.6 between the predicted and observed values.

In fact, in addition to the subsurface ocean heat condition, the atmosphere also plays an important role in forcing the ENSO system. For example, the westerly wind burst, an intraseasonal phenomenon occurring in the equatorial western and central Pacific, is widely believed to be an important trigger for El Niño events^{11–15}. Based on numerical experiments, it has been shown that, with the same initial ocean heat content along the equatorial Pacific, an additional westerly wind burst during the boreal spring could change an original neutral event into an El Niño event¹⁵. This suggests that we need to extract the exact information from both the ocean and the atmosphere during the boreal spring to be able to predict the ENSO events and reduce the SPB. We show here that it is possible to successfully predict ENSO starting from the boreal spring using a simple linear regression method that considers the variations in both air–sea components.

The first predictor for the ENSO system is the oceanic heat content along the equatorial Pacific, which is defined here as the basin mean (120° E–80° W, 2° S–2° N) TCD anomalies (TCDa_M hereinafter). According to the recharge paradigm, the progress of the oceanic heat content from accumulation to release (i.e., discharge) is important in the development of El Niño, and the recharge progress (i.e., from release to accumulation) is

Department of Atmospheric and Oceanic Sciences & Institute of Atmospheric Sciences, Fudan University, Shanghai, China. Correspondence and requests for materials should be addressed to X.-H.F. (email: fangxh@fudan.edu.cn)

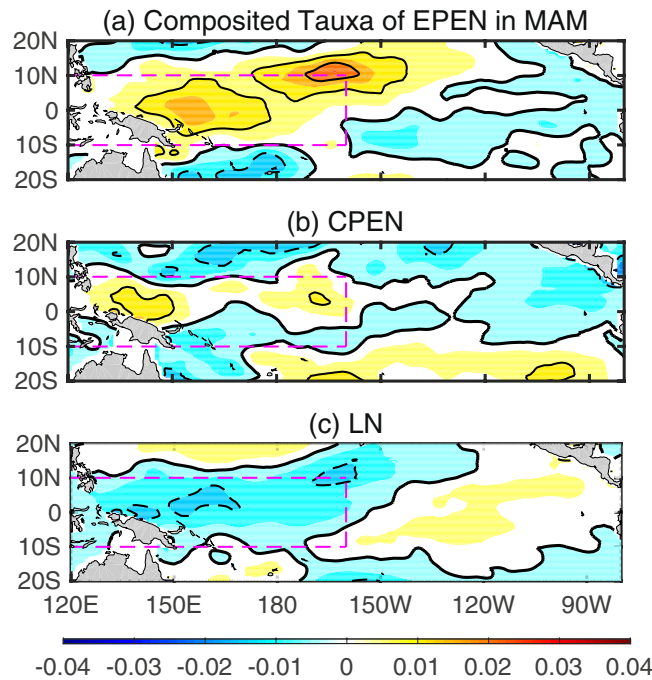


Figure 1. Composite mean Tauxa of the ENSO events during the boreal spring (March–May). (a) EP El Niño. (b) CP El Niño. (c) La Niña. The contour interval is 0.01 N/m². The purple box represents the region (120° E–160° W, 10° S–10° N).

important in the development of La Niña^{5,16,17}. However, we cannot give an accurate prediction of the ENSO during the boreal spring based on this information alone. The correlation coefficient between the TCDA_M index during the boreal spring (March–May) and the Niño3.4 SST anomaly index during the boreal winter (October–December) is only 0.56 for the period 1980–2016 (see Figure S1 in the supplementary information). Although passing the 95% confidence level using Student's *t*-test with 18 degrees of freedom, this relatively low value indicates that the discharging (recharging) process during the boreal spring is not a sufficient condition for leading the occurrence of El Niño (La Niña) events. Information from the atmosphere should also be considered.

Figure 1 shows the composite mean of the anomalous zonal wind stress (Tauxa) of the EP El Niño (the canonical El Niño with the maximum SST anomalies located in the EP), central Pacific (CP) El Niño (the new type of El Niño with maximum warming anomalies confined mostly in the CP) and La Niña events during the boreal spring. Although different types of ENSO make the distribution of SST anomalies complex, the westerly (easterly) Tauxa during El Niño (La Niña) events are concentrated in similar regions over the tropical western Pacific (the purple box in Fig. 1). Physically, these anomalous zonal wind stresses could stimulate Kelvin waves on the oceanic TCD and the thermally coupled Walker mode on the oceanic surface to trigger the ENSO event^{18–22}. The thermally coupled Walker mode is used by ref.¹⁸ to refer the Southern Oscillation mode of variability that emerges from the thermodynamic coupling to an ocean mixed layer, i.e., without dynamical coupling to the ocean. The high correlation coefficient between the box mean Tauxa (Tauxa_W hereinafter) during the boreal spring and the Niño3.4 SST anomaly index during the boreal winter is 0.71 for the period 1980–2016 and passes the 95% confidence level using Student's *t*-test with 19 degrees of freedom, confirming the important role played by the atmosphere. This also indicates that the Tauxa_W index during the boreal spring could be another good predictor of the ENSO events. It is encouraging that the TCDA_M and Tauxa_W indices during the boreal spring are linearly independent, i.e., their correlation coefficient during 1980–2016 is only 0.15. As a result, we believe that a bivariate linear regression model using the TCDA_M and Tauxa_W indices during the boreal spring could give a more accurate prediction of ENSO for the following seasons than a model that relies on any one predictor.

Based on this simple model, the predicted SST anomalies during the boreal winter over the equatorial central-eastern Pacific are similar to the observations for the period 1980–2016, i.e., the correlation coefficients are 0.84, 0.85 and 0.71 for the Niño3.4, Niño3 (150° W–90° W, 5° S–5° N) and Niño4 (160° E–150° W, 5° S–5° N) indices, respectively. They all pass the 95% confidence level using Student's *t*-test. Meanwhile, the regression coefficients of the TCDA_M and Tauxa_W indices are 0.55 ± 0.23 and 0.76 ± 0.23 , respectively. They represent the relative contribution of the ocean and atmosphere to the evolution of ENSO and are denoted by 95% confidence intervals using Student's *t*-test. It indicates that the combined role of the oceanic and atmospheric parts during the boreal spring is required to induce an ENSO event and ignoring either one of these parts will severely reduce the prediction skills of the model.

Considering the role of the TCDA_M index in predicting ENSO decreased suddenly from 1980–1999 to 2000–2016^{23,24}, i.e., a decadal variation, the bivariate linear regression models are therefore constructed separately for these two periods. Then these two models are used to predict the following evolution of ENSO during 1980–1999 and 2000–2016, respectively. Figure 2 shows the total predicted results, i.e., 1980–2016. The correlation

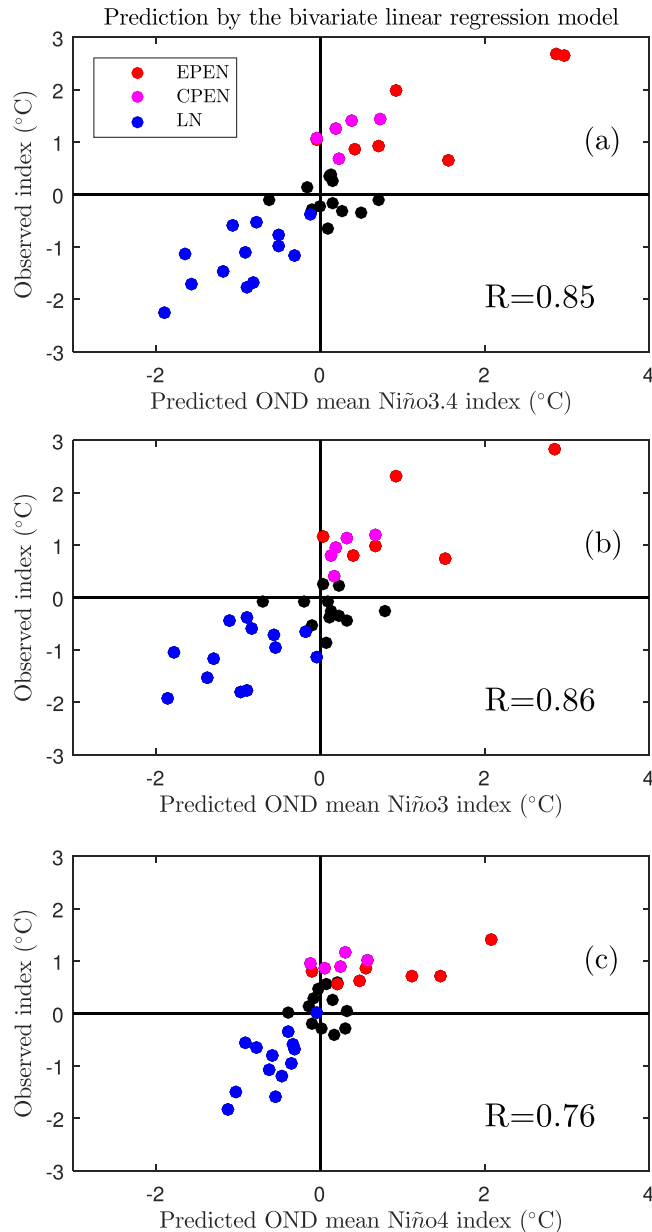


Figure 2. Relations between the predicted and observed Niño indices during the boreal winter. The predicted indices are obtained by the bivariate linear regression method using the TCDa_M and Tauxa_W indices during the boreal spring as the predictors. Panels (a–c) are for the Niño3.4, Niño3 and Niño4 indices, respectively. In each panel, the red, purple and blue dots are for the eastern Pacific El Niño, the central Pacific El Niño and La Niña events, respectively, whereas the black dots are for neutral years. The correlation coefficients between the predicted and observed Niño indices are also shown in each panel. OND represents the boreal winter season, i.e., October, November and December.

coefficients between the predicted and observed Niño3.4, Niño3 and Niño4 indices during the boreal winter are as high as 0.85, 0.86 and 0.76, respectively. Besides, apart from the two El Niño events, i.e., 1987–1988 and 1994–1995, all the ENSO types are successfully predicted during the boreal spring, i.e., El Niño and La Niña events are located in the first and third quadrants, respectively. The change in the regression coefficients also shows that although the contribution from the TCDa_M (0.64 ± 0.40) and Tauxa_W (0.59 ± 0.40) indices are almost equivalent during the first period, the Tauxa_W index (0.95 ± 0.33) plays a dominant role over the TCDa_M index (0.47 ± 0.33) in predicting the ENSO events during the more recent period. This indicates that more information about the ENSO system is contained in the atmosphere than in the ocean during the boreal spring in the 2000–2016 period. On the one hand, these changes are consistent with the argument from ref.²³ that the role of the TCDa_M index in predicting ENSO decreased suddenly from 1980–1999 to 2000–2016. On the other hand, they are consistent with the fact that the central Pacific type of El Niño occurred more frequently during the

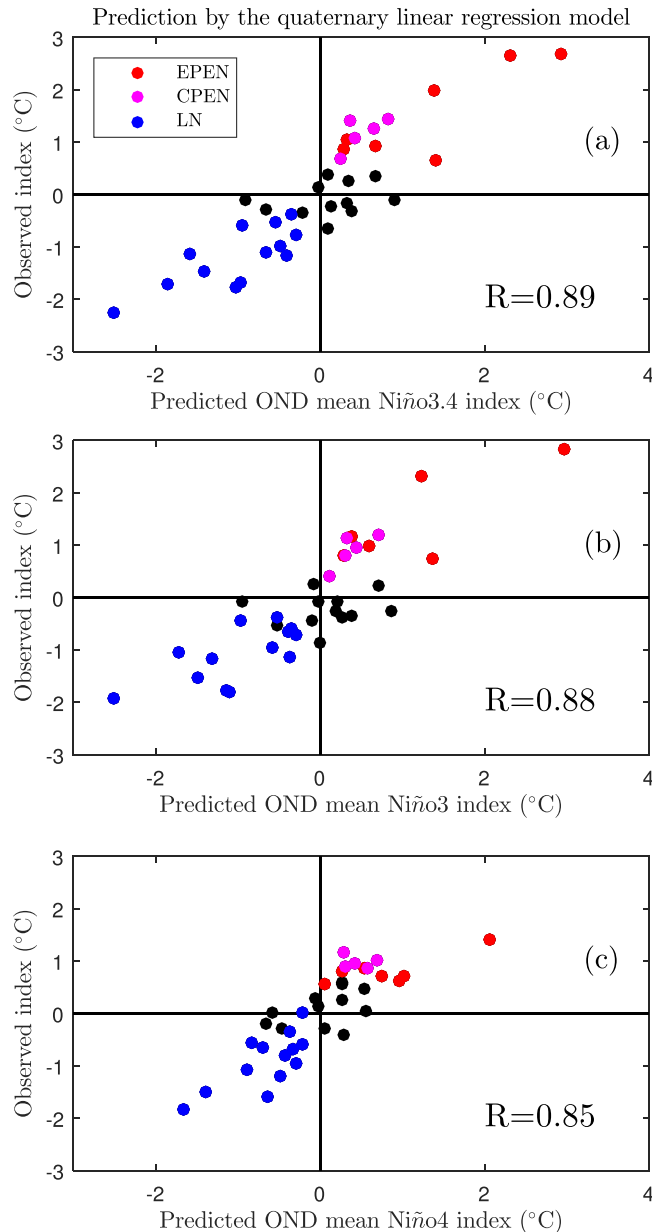


Figure 3. Relations between the predicted and observed Niño indices during the boreal winter. The predicted indices are obtained by the quaternary linear regression method that using the TCDA_M, Tauxa_W, central Pacific and eastern Pacific indices during the boreal spring. Panels (a–c) are for the Niño3.4, Niño3 and Niño4 indices, respectively. In each panel, the red, purple and blue dots are for the eastern Pacific El Niño, the central Pacific El Niño and La Niña events, respectively, whereas the black dots are for neutral years. The correlation coefficients between the predicted and observed Niño indices are also shown in each panel. OND represents the boreal winter season, i.e., October, November and December.

recent decade, for which the dominant dynamic processes are the zonal advective feedback and the latent heat feedback^{25,26}, which are both related with the zonal wind anomalies over the western and central Pacific region.

Since the concept of two types of El Niño event first emerged^{27–31}, the complexity and uncertainty of ENSO have increased^{32–34}. To utilize the SST information and take the different types of ENSO into account, we further add the CP and EP indices²⁸ into the predictors during the boreal spring, i.e., we construct a quaternary linear regression model to predict the boreal winter El Niño indices. Again, the separate models are constructed for the periods 1980–1999 and 2000–2016, respectively, and these two models are used to predict the following evolution of ENSO during their corresponding periods. The total predicted results (i.e., 1980–2016) are shown in Fig. 3. We obtain an improved prediction, especially for the Niño4 index, when the correlation coefficient between the prediction and observations is as high as 0.85. All the different types of ENSO are now successfully predicted during the boreal spring. This means that by considering the SST of the two types of ENSO events during the boreal spring, the SST anomalies over the equatorial central–eastern Pacific region during the boreal winter can be predicted successfully.

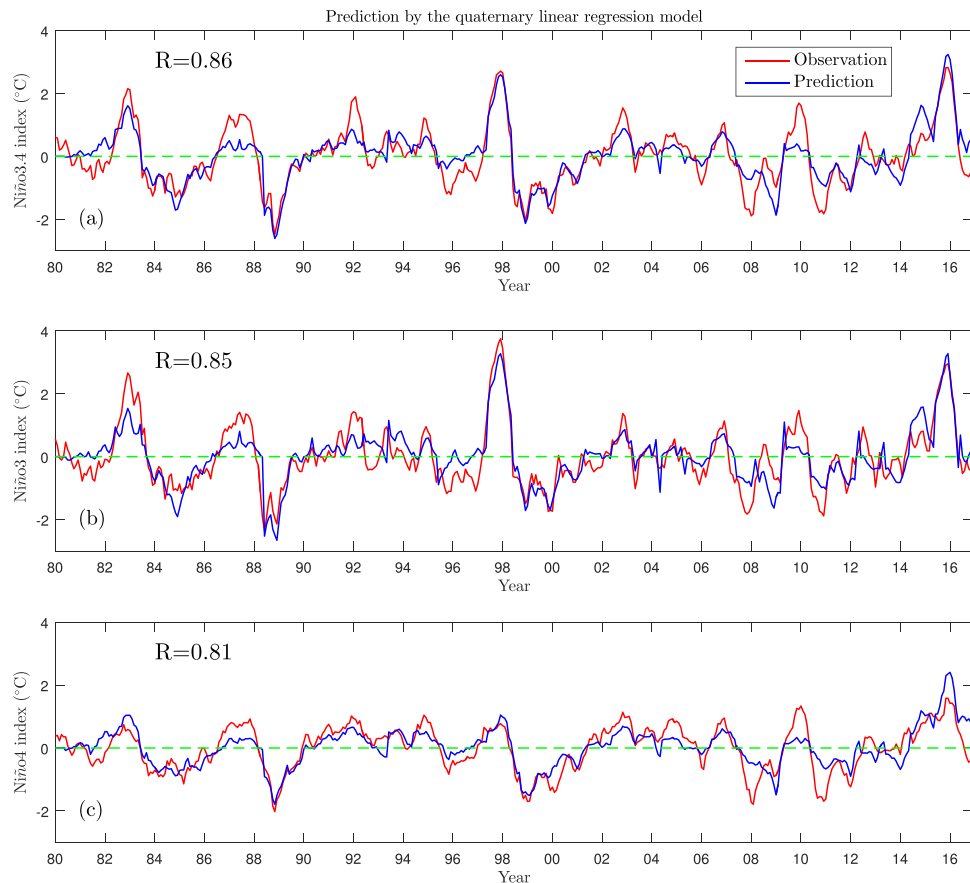


Figure 4. Retrospective predictions of the El Niño indices in each month from June 1980 to December 2016. Panels (a–c) are for the Niño3.4, Niño3 and Niño4 indices, respectively. In each panel, the red lines are for the observed indices and the blue lines are the predictions (from June to the following May of each year) using the quaternary linear regression method using the TCDA_M, Tauxa_W, central Pacific and eastern Pacific indices during the boreal spring. The correlation coefficients between the predicted and observed El Niño indices are also shown in each panel.

The contribution rates of the four indices during the two periods show that the dominant predictors are still the TCDA_M index during 1980–1999 and the Tauxa_W index during 2000–2016. Taking the Niño3.4 index prediction as an example, the regression coefficients of the TCDA_M, Tauxa_W, CP and EP indices during the period 1980–1999 are 0.98 ± 0.46 , 0.25 ± 0.43 , 0.65 ± 0.49 and 0.54 ± 0.51 , respectively. During the period 2000–2016, these regression coefficients are 0.36 ± 0.46 , 1.05 ± 0.43 , -0.14 ± 0.76 and 0.1 ± 0.65 , respectively. This confirms that the main frame structure of the ENSO system could be mostly controlled by variations in the oceanic heat content along the equatorial Pacific and the zonal wind stress over the tropical western Pacific and that their relative roles have significant decadal variations.

Using the quaternary linear regression method, the SST anomalies from June to the following May of each year can all be predicted based on information from the boreal spring. Figure 4 shows the predicted and observed El Niño indices of all the months from June 1980 to December 2016. The predictions are quite similar to the observations, except for the prediction of the intensity of ENSO in some years—for example, the predicted 2007–2008 and 2010–2011 La Niña and the 1986–1988 and 2009–2010 El Niño events are too weak, whereas the 2014–2015 El Niño event is too strong. The correlation coefficients of the Niño3.4, Niño3 and Niño4 indices in the period 1980–2016 are as high as 0.86, 0.85 and 0.81, respectively. Thus if we take the information from both the ocean and atmosphere during the boreal spring into right consideration, the subsequent evolution of air–sea interactions over the equatorial Pacific (the ENSO events) can be largely predicted.

In summary, although remarkable achievements have been made in the simulation and prediction of the ENSO events, the skill for predicting ENSO starting from the boreal spring is still poor, making predictions from a long lead time difficult. Because the memory of the ocean is much longer than that of the atmosphere, the prediction of the ENSO events is considered to be dominated by oceanic processes. This has led to the classic ENSO paradigms—the delayed oscillator^{35,36} and the recharging oscillator—that consider the ENSO phenomenon as a slightly damped periodic oscillation modulated by stochastic noise^{37–39}. However, recent work has found that, with the same distribution of the oceanic subsurface temperature, an additional westerly wind burst during the boreal spring could change the original neutral event into an El Niño event. This suggests that the ENSO system starting in the boreal spring does not only rely on the oceanic heat content and that exact information from the

atmosphere is also crucial. This has been especially true during recent decades, when the part played by the oceanic heat content in predicting the ENSO events has shown a sudden decrease.

We extracted information from both the ocean and atmosphere during the boreal spring, i.e., the TCDa_M index that representing the oceanic heat content, the Tauxa_W index that representing the atmospheric forcing, the CP and EP indices that representing the SST distribution for the two types of ENSO events. We then used a quaternary linear regression method to predict the subsequent SST anomalies over the equatorial Pacific from June to the following May. The correlation coefficients between the predicted and observed SST anomalies over the equatorial central–eastern Pacific were >0.81 for the period 1980–2016 and all the different types of ENSO were successfully predicted during the boreal spring. The success of the retrospective prediction relies mainly on the TCDa_M and Tauxa_W indices and their relative contributions have significant decadal variations. It is interesting to note that a similar successful statistical model was also constructed recently to overcome the SPB issue of the ENSO forecast⁴⁰. Different from the two predictors used in our work, the oceanic predictor in their model is the potential temperature anomalies over the 130° E–180°, 5° N–5° S, 5–250 m area and the atmospheric predictor is the cumulative zonal wind anomalies over the 140° E–160° W, 5° N–5° S area and integrated from November up to the prediction month. But consistently, the two successful models both deeply rely on the information from both the ocean and atmosphere during the boreal spring.

These results indicate that to predict the ENSO events with a longer lead time, i.e., largely reducing the SPB, variations in both the ocean and atmosphere during the boreal spring should be well predicted first. It should be emphasized that the TCDa_M and Tauxa_W indices used in this article represent different mechanisms for the evolution of the ENSO system. Specifically, the TCDa_M index mainly reflects the classic ENSO perspective (e.g., the delayed oscillator and recharging oscillator), which treat the ENSO system as a linear oscillating phenomenon based on the wave dynamics and the water exchange between the equatorial and off-equatorial regions, respectively. While the Tauxa_W index in the boreal spring (the weakest air–sea interaction over the equatorial Pacific during a year), which can stimulate Kelvin waves on the oceanic TCD and the thermally coupled Walker mode on the oceanic surface to influence the ENSO evolution, mainly reflects the influences beyond the linear oscillating framework. This includes the signals from the westerly wind burst (WVB)^{12,14}, signals from the northeast^{41–43} and southeast Pacific⁴⁶ through the seasonal footprinting mechanism and signals from the Indian Ocean⁴⁷ and Atlantic Ocean^{48–51} through anomalous atmospheric circulation and waves, etc. The decadal variations of the relative contributions of the TCDa_M and Tauxa_W indices indicate the different importance of their related physical processes, e.g., the influences beyond the linear oscillating framework is more important in the recent decade for reducing the SPB. In addition, the main periods of the TCDa_M and Tauxa_W indices are 3.7 and 2.5 years, respectively (figures not shown). This difference gives us a clue to investigate the essence of the wide range of the ENSO irregular period (generally 2–7 years)³⁸, and also the decadal variations of the ENSO variability and frequencies^{52,53}.

Methods

Datasets. The observational and reanalysis datasets were obtained from the National Centers for Environmental Prediction Global Ocean Data Assimilation System (GODAS)⁵⁴. The datasets were analysed for the period 1980–2016 and the mean seasonal cycles were removed to calculate the anomalies in each field. The equatorial TCD was defined as the depth at which the oceanic potential temperature was 20 °C. The TCDa_M index, which represents the oceanic heat content in the equatorial Pacific, was calculated as the area mean of the TCD anomalies in the region (120° E–80° W, 2° S–2° N). The Tauxa_W index was calculated by the area mean of Tauxa over the region (120° E–160° W, 10° S–10° N). The CP and EP indices were calculated based on the regression-empirical orthogonal function method introduced in ref.²⁷. The TCDa_M, Tauxa_W, CP and EP indices were all standardized before they were used to construct the linear regression model.

Bivariate linear regression model. To predict the winter El Niño indices based on the air–sea information during the boreal spring, we first constructed a bivariate linear regression model. The model is as follows:

$$Nino_p^{OND} = a \times TCDa_M_o^{MAM} + b \times Tauxa_W_o^{MAM} + c \quad (1)$$

where $Nino_p^{OND}$ is the predicted El Niño index in the boreal winter (October–December) and $TCDa_M_o^{MAM}$ and $Tauxa_W_o^{MAM}$ are the observed TCDa_M and Tauxa_W indices during the boreal spring (March–May), respectively. a , b and c are the regression coefficients and are obtained by replacing $Nino_p^{OND}$ with the observed Niño index in the boreal winter. This regression method was used to predict all the El Niño indices separately.

Quaternary linear regression model. This is similar to the bivariate linear regression model, but with the addition of the CP and EP indices during the boreal spring:

$$Nino_p^{OND} = a \times TCDa_M_o^{MAM} + b \times Tauxa_W_o^{MAM} + c \times CP_o^{MAM} + d \times EP_o^{MAM} + e \quad (2)$$

where CP_o^{MAM} and EP_o^{MAM} are the observed CP and EP indices during the boreal spring, respectively. a , b , c , d and e are the regression coefficients obtained by replacing $Nino_p^{OND}$ with the observed Niño index in the boreal winter. The model used to predict the SST anomalies over the equatorial Pacific from June to the following May during each year was constructed using a similar method with the term on the left-hand side replaced by the SST anomalies in each month.

Statistical analysis. Because the data from the geophysical time series are not always independent of each other, the persistence and the finite size of the samples must be considered when computing the statistics^{55,56}. In this method, the degrees of freedom can be derived for significance tests using the correlation between two time series (X_i and Y_i) with different autocorrelation sequences of ρ_τ^X and ρ_τ^Y as follows⁵⁶:

$$T_{XY}^* = \frac{T}{\sum_{\tau=-T}^{T-1} (1 - |\tau|/T) \rho_\tau^X \rho_\tau^Y} \quad (3)$$

where T_{XY}^* is the number of degrees of freedom used in the significance calculation and T is the unadjusted number of degrees of freedom.

References

- Alexander, M. A. *et al.* The atmospheric bridge: the influence of ENSO teleconnections on air-sea interaction over the global oceans. *Journal of Climate* **15**, 2205–2231 (2002).
- Jin, F.-F. An equatorial ocean recharge paradigm for ENSO. Part I: conceptual model. *Journal of Atmospheric Sciences* **54**, 811–829 (1997).
- Jin, F.-F. An equatorial ocean recharge paradigm for ENSO. Part II: a stripped-down coupled model. *Journal of the Atmospheric Sciences* **54**, 830–847 (1997).
- McPhaden, M. J. Tropical Pacific Ocean heat content variations and ENSO persistence barriers. *Geophysical Research Letters* **30**, 1480, <https://doi.org/10.1029/2003GL016872> (2003).
- Ramesh, N. & Murtugudde, R. All flavours of El Niño have similar early subsurface origins. *Nature Climate Change* **3**, 42–46, <https://doi.org/10.1038/NCLIMATE1600> (2012).
- Clarke, A. J. El Niño Physics and El Niño Predictability. *Annual Review of Marine Science* **6**, 79–99, <https://doi.org/10.1146/annurev-marine-010213-135026> (2014).
- Masuda, S. *et al.* A new approach to El Niño prediction beyond the spring season. *Scientific Reports* **5**, 16782, <https://doi.org/10.1038/srep16782> (2015).
- Mu, M., Xu, H. & Duan, W.-S. A kind of initial errors related to “spring predictability barrier” for El Niño events in Zebiak-Cane model. *Geophysical Research Letters* **34**, L03709, <https://doi.org/10.1029/2006GL027412> (2007).
- Webster, P. J. & Yang, S. Monsoon and Enso: selectively interactive systems. *Quarterly Journal of the Royal Meteorological Society* **118**, 877–926 (1992).
- Barnston, A. G., Tippett, M. K., L’Heureux, M. L., Li, S.-H. & Dewitt, D. G. Skill of real-time seasonal ENSO model predictions during 2002–11: is our capability increasing? *Bulletin of the American Meteorological Society* **93**, 631–651, <https://doi.org/10.1175/BAMS-D-11-00111.1> (2012).
- Chen, D.-K. *et al.* Strong influence of westerly wind bursts on El Niño diversity. *Nature Geoscience* **8**, 339–345, <https://doi.org/10.1038/NGEO2399> (2015).
- Fedorov, A. V., Hu, S.-N., Lengaigne, M. & Guilyardi, E. The impact of westerly wind bursts and ocean initial state on the development, and diversity of El Niño events. *Climate Dynamics* **44**, 1381–1401, <https://doi.org/10.1007/s00382-014-2126-4> (2015).
- Gebbie, G., Eisenman, I., Wittenberg, A. & Tziperman, E. Modulation of westerly wind bursts by sea surface temperature: a semistochastic feedback for ENSO. *Journal of Atmospheric Sciences* **64**, 3281–3295, <https://doi.org/10.1175/JAS4029.1> (2007).
- Hu, S.-N., Fedorov, A. V., Lengaigne, M. & Guilyardi, E. The impact of westerly wind bursts on the diversity and predictability of El Niño events: An ocean energetics perspective. *Geophysical Research Letters* **41**, 4654–4663, <https://doi.org/10.1002/2014GL059573> (2014).
- Menkes, C. E. *et al.* About the role of Westerly Wind Events in the possible development of an El Niño in 2014. *Geophysical Research Letters* **41**, 6476–6483, <https://doi.org/10.1002/2014GL061186> (2014).
- Ballester, J. *et al.* Sensitivity of El Niño intensity and timing to preceding subsurface heat magnitude. *Scientific Reports* **6**, 36344, <https://doi.org/10.1038/srep36344> (2016).
- Ballester, J., Petrova, D., Bordoni, S., Cash, B. & Rodó, X. Timing of subsurface heat magnitude for the growth of El Niño events. *Geophysical Research Letters* **44**, 8501–8509, <https://doi.org/10.1002/2017GL074557> (2017).
- Clement, A., Dinezio, P. & Deser, C. Rethinking the ocean’s role in the Southern Oscillation. *Journal of Climate* **24**, 4056–4072, <https://doi.org/10.1175/2011JCLI3973.1> (2011).
- Hendon, H. H., Liebmann, B. & Glick, J. D. Oceanic Kelvin waves and the Madden-Julian Oscillation. *Journal of the Atmospheric Sciences* **55**, 88–101 (1998).
- Kessler, W. S., McPhaden, M. J. & Weickmann, K. M. Forcing of intraseasonal Kelvin waves in the equatorial Pacific. *Journal of Geophysical Research: Oceans* **100**, 10613–10631 (1995).
- Kutsuwada, K. & McPhaden, M. J. Intraseasonal variations in the upper equatorial Pacific Ocean prior to and during the 1997–98 El Niño. *Journal of Physical Oceanography* **32**, 1133–1149 (2002).
- Wyrtki, K. El Niño—the dynamic response of the equatorial Pacific ocean to atmospheric forcing. *Journal of Physical Oceanography* **5**, 572–583 (1975).
- Hu, Z.-Z. *et al.* On the Shortening of the Lead Time of Ocean Warm Water Volume to ENSO SST Since 2000. *Scientific Reports* **7**, <https://doi.org/10.1038/s41598-017-04566-z> (2017).
- Zheng, F., Fang, X. H., Zhu, J., Yu, J. Y. & Li, X. C. Modulation of Bjerknes feedback on the decadal variations in ENSO predictability. *Geophysical Research Letters* **43**, 12,560–12,568, <https://doi.org/10.1002/2016GL071636> (2016).
- Yeh, S.-W., Kug, J.-S. & An, S.-I. Recent progress on two types of El Niño: Observations, dynamics, and future changes. *Asia-Pacific Journal of Atmospheric Sciences* **50**, 69–81, <https://doi.org/10.1007/s13143-014-0028-3> (2014).
- Fang, X.-H. & Zheng, F. Simulating Eastern- and Central-Pacific Type ENSO Using a Simple Coupled Model. *Advances in Atmospheric Sciences* **35**, 671–681, <https://doi.org/10.1007/s00376-017-7209-9> (2018).
- Ashok, K., Behera, S. K., Rao, S. A., Weng, H. & Yamagata, T. El Niño Modoki and its possible teleconnection. *Journal of Geophysical Research Oceans* **112**, C11007, <https://doi.org/10.1029/2006JC003798> (2007).
- Kao, H. Y. & Yu, J.-Y. Contrasting eastern-Pacific and central-Pacific types of ENSO. *Journal of Climate* **22**, 615–632, <https://doi.org/10.1175/2008JCLI2309.1> (2009).
- Kug, J.-S., Jin, F.-F. & An, S.-I. Two types of El Niño events: cold tongue El Niño and warm pool El Niño. *Journal of Climate* **22**, 1499–1515, <https://doi.org/10.1175/2008JCLI2624.1> (2009).
- Larkin, N. K. & Harrison, D. E. Global seasonal temperature and precipitation anomalies during El Niño autumn and winter. *Geophysical Research Letters* **32**, L16705, <https://doi.org/10.1029/2005GL022860> (2005).
- Yu, J. Y. & Kao, H. Y. Decadal changes of ENSO persistence barrier in SST and ocean heat content indices: 1958–2001. *Journal of Geophysical Research Atmospheres* **112**, 125–138, <https://doi.org/10.1029/2006JD007654> (2007).
- Zheng, F., Fang, X.-H., Yu, J.-Y. & Zhu, J. Asymmetry of the Bjerknes positive feedback between the two types of El Niño. *Geophysical Research Letters* **41**, 7651–7657, <https://doi.org/10.1002/2014GL062125> (2014).

33. Fang, X.-H., Zheng, F. & Zhu, J. The cloud-radiative effect when simulating strength asymmetry in two types of El Niño events using CMIP5 models. *Journal of Geophysical Research Oceans* **120**, 4357–4369, <https://doi.org/10.1002/2014JC010683> (2015).
34. Zheng, F. & Yu, J.-Y. Contrasting the skills and biases of deterministic predictions for the two types of El Niño. *Advances in Atmospheric Sciences* **34**, 1395–1403, <https://doi.org/10.1007/s00376-017-6324-y> (2017).
35. Schopf, P. S. & Suarez, M. J. Vacillations in a coupled ocean–atmosphere model. *Journal of the Atmospheric Sciences* **45**, 549–568 (1988).
36. Suarez, M. J. & Schopf, P. S. A delayed action oscillator for ENSO. *Journal of the Atmospheric Sciences* **45**, 3283–3287 (1988).
37. Chen, D. & Cane, M. A. El Niño prediction and predictability. *Journal of Computational Physics* **227**, 3625–3640, <https://doi.org/10.1016/j.jcp.2007.05.014> (2008).
38. Wang, C.-Z. & Picaut, J. In *Earth's Climate: The Ocean-Atmosphere Interaction* Vol. 147 *Geophysical Monograph Series* (eds Chun-Zai Wang, Shang-Ping Xie & James A. Carton) 21–48 (AGU, 2004).
39. Fang, X.-H. & Mu, M. A three-region conceptual model for central Pacific El Niño including zonal advective feedback. *Journal of Climate* **31**, 4965–4979, <https://doi.org/10.1175/JCLI-D-17-0633.1> (2018).
40. Lai, A. W.-C., Herzog, M. & Graf, H.-F. ENSO forecasts near the spring predictability barrier and possible reasons for the recently reduced predictability. *Journal of Climate* **31**, 815–838, <https://doi.org/10.1175/JCLI-D-17-0180.1> (2018).
41. Vimont, D. J., Battisti, D. S. & Hirst, A. C. Footprinting: A seasonal connection between the tropics and mid-latitudes. *Geophysical Research Letters* **28**, 3923–3926 (2001).
42. Vimont, D. J., Wallace, J. M. & Battisti, D. S. The seasonal footprinting mechanism in the Pacific: implications for ENSO. *Journal of Climate* **16**, 2668–2675 (2003).
43. Yu, J.-Y., Kao, H.-Y. & Lee, T. Subtropics-related interannual sea surface temperature variability in the central equatorial Pacific. *Journal of Climate* **23**, 2869–2884, <https://doi.org/10.1175/2010JCLI3171.1> (2010).
44. Yeh, S.-W., Wang, X., Wang, C.-Z. & Dewitt, B. On the relationship between the North Pacific Climate Variability and the Central Pacific El Niño. *Journal of Climate* **28**, 663–677, <https://doi.org/10.1175/JCLI-D-14-00137.1> (2015).
45. Wang, X., Chen, M.-Y., Wang, C.-Z., Yeh, S.-W. & Tan, W. Evaluation of performance of CMIP5 models in simulating the North Pacific Oscillation and El Niño Modoki. *Climate Dynamics*, <https://doi.org/10.1007/s00382-018-4196-1> (2018).
46. Zhang, H.-H., Clement, A. & Nezio, P. D. The south Pacific meridional mode: a mechanism for ENSO-like variability. *Journal of Climate* **27**, 769–783, <https://doi.org/10.1175/JCLI-D-13-00082.1> (2014).
47. Izumo, T. *et al.* Influence of Indian Ocean Dipole and Pacific recharge on following year's El Niño: interdecadal robustness. *Climate Dynamics* **42**, 291–310, <https://doi.org/10.1007/s00382-012-1628-1> (2014).
48. Ham, Y. G., Kug, J. S. & Park, J. Y. Two distinct roles of Atlantic SSTs in ENSO variability: North Tropical Atlantic SST and Atlantic Niño. *Geophysical Research Letters* **40**, 4012–4017, <https://doi.org/10.1002/grl.50729> (2013).
49. Ham, Y.-G., Kug, J.-S., Park, J.-Y. & Jin, F.-F. Sea surface temperature in the north tropical Atlantic as a trigger for El Niño/Southern Oscillation events. *Nature Geoscience* **6**, 112–116, <https://doi.org/10.1038/NGEO1686> (2013).
50. Wang, X., Wang, C.-Z., Zhou, W., Wang, D.-X. & Song, J. Teleconnected influence of North Atlantic sea surface temperature on the El Niño onset. *Climate Dynamics* **37**, 663–676, <https://doi.org/10.1007/s00382-010-0833-z> (2011).
51. Wang, X., Wang, C.-Z., Zhou, W., Liu, L. & Wang, D.-X. Remote influence of North Atlantic SST on the equatorial westerly wind anomalies in the western Pacific for initiating an El Niño event: an Atmospheric General Circulation Model Study. *Atmospheric Science Letters* **14**, 107–111, <https://doi.org/10.1002/asl2.425> (2013).
52. Hu, Z.-Z. *et al.* Weakened interannual variability in the tropical Pacific Ocean since 2000. *Journal of Climate* **26**, 2601–2613, <https://doi.org/10.1175/JCLI-D-12-00265.1> (2013).
53. McPhaden, M. J. A 21st century shift in the relationship between ENSO SST and warm water volume anomalies. *Geophysical Research Letters* **39**, L09706, <https://doi.org/10.1029/2012GL051826> (2012).
54. Behringer, D. & Xue, Y. In *Eighth Symposium on Integrated Observing and Assimilation Systems for Atmosphere, Oceans, and Land Surface*. AMS 84th Annual Meeting (Washington State Convention and Trade Center, Seattle, Washington, 2004).
55. Trenberth, K. E. Some effects of finite sample size and persistence on meteorological statistics. *Part I: autocorrelations*. *Monthly Weather Review* **112**, 2369–2379 (1984).
56. Bretherton, C. S., Widmann, M., Dymnikov, V. P., Wallace, J. M. & Bladé, I. The effective number of spatial degrees of freedom of a time-varying field. *Journal of Climate* **12**, 1990–2009 (1999).

Acknowledgements

This work was supported by the Project funded by China Postdoctoral Science Foundation (Grant No. 2017M610225).

Author Contributions

X.-H.F. did the analysis wrote this paper. M.M. contributed to discussions and manuscript.

Additional Information

Supplementary information accompanies this paper at <https://doi.org/10.1038/s41598-018-28964-z>.

Competing Interests: The authors declare no competing interests.

Publisher's note: Springer Nature remains neutral with regard to jurisdictional claims in published maps and institutional affiliations.



Open Access This article is licensed under a Creative Commons Attribution 4.0 International License, which permits use, sharing, adaptation, distribution and reproduction in any medium or format, as long as you give appropriate credit to the original author(s) and the source, provide a link to the Creative Commons license, and indicate if changes were made. The images or other third party material in this article are included in the article's Creative Commons license, unless indicated otherwise in a credit line to the material. If material is not included in the article's Creative Commons license and your intended use is not permitted by statutory regulation or exceeds the permitted use, you will need to obtain permission directly from the copyright holder. To view a copy of this license, visit <http://creativecommons.org/licenses/by/4.0/>.

© The Author(s) 2018